A New Analysis Scheme for Complex Forced Rayleigh Scattering Profiles

Sangsoo Park,† Hyuk Yu,*,† and Taihyun Chang*,‡

Department of Chemistry, University of Wisconsin, Madison, Wisconsin 53706, and Department of Chemistry, Pohang Institute of Science and Technology (POSTECH), P.O. Box 125, Pohang, 790-600, Republic of Korea

Received January 4, 1993; Revised Manuscript Received March 11, 1993

ABSTRACT: A recently proposed mechanism for complex signal profiles of forced Rayleigh scattering (Park et al. *J. Phys. Chem.* **1991**, *95*, 7121) is tested with a system of globular protein–surfactant complexes. The mechanism starts with a hypothesis of double grating of pure phase complementarity which is shown to produce extreme departures, such as decay–growth–decay type, from single exponential decay. A new analysis scheme for such a complex signal type is proposed, and it has been validated here experimentally with the dynamic light scattering results in conjunction with the FRS measurements.

Introduction

Forced Rayleigh scattering (FRS) utilizes a transient optical grating induced by periodic concentration profile of a photoresponsive moiety imprinted on the specimen either by crossing two coherent laser beams[1-8,10-19] or by masking the excitation source with a Ronchi ruling.[9] The difference in optical properties, absorptivity or refractive index, of shifted (isomerized) and unshifted states for a photochromic or photobleachable (irreversibly isomerized) label results in a diffraction of the reading beam.[7,8] The diffracted intensity decays with time by two principal mechanisms, i.e., the mass diffusion and the spontaneous thermal reconversion of shifted state of the label; hence, the diffusion coefficient and shifted-state lifetime can be determined from the analysis of the decay profile.[2,3,10] If the concentration profile decays via the Fickian diffusion process, and if the shifted-state label has the same diffusion coefficient as that of the unshifted one, the diffraction intensity decays exponentially. Frequently, however, deviations from single exponential decay are observed,[11-19] and they were ascribed to the presence of a pair of the complementary gratings which consists of excess optically shifted and unshifted states of the photolabel.[1,11-13,17,19] If the diffusion coefficients of the two states of the photoprobe by itself or as labeled to a larger molecule are different, the optical fields diffracted from individual grating decays in different rates and their mutual interference gives rise to the observed decay profiles, which are no longer single exponential and in some cases even significantly depart from a nonexponential but monotonic decay.

An extreme departure from a single exponential is a decay–growth–decay type signal. This type of signal was reported first by Rhee et al.[11] When they labeled bovine serum albumin (BSA) with a benzospiropyran, the FRS signals from this sample showed maxima and minima instead of the usual single exponential decay. The same group also reported this type of signal from human immunoglobulin G (IgG) labeled with 5-isothiocyanatofluorescein (FITC) and *p*-isothiocyanatoazobenzene (ABITC).[12] They attributed these signals to the aggregation or dissociation of the proteins following the photoexcitation of the labels. On the other hand, the same type of signals was also observed with the diffusion of probe dyes in highly concentrated polymer solutions and in bulk polymers. Wang and co-workers reported that the FRS signals from camphoquinone (CQ) in polystyrene (PS),[13] poly(methyl methacrylate) (PMMA),[14,15] and polycarbonate (PC)[16] also show the abnormal decay shape. Huang et al.[17] reported that the signal from a pH indicator dye, methyl red, in polystyrene solution is a single exponential up to 85 wt % polymer but changes to the decay–growth–decay type at higher polymer concentration. The authors attributed the appearance of these signals to the difference in diffusion coefficients of the shifted and unshifted probes in a rigid environment where the size of free void volume is comparable to that of the probe dye. Lastly, this abnormal signal shape was observed in probe diffusion experiments in H-bonding polymer solutions at low polymer concentration. Lee and Lodge[18] reported the abnormal signal shape from methyl red in poly(vinyl acetate) (PVAc) solutions, and Lee et al.[19] observed it in PMMA solutions. Methyl red is suspected to interact with PVAc and PMMA by H-bonding, and a difference in the binding constants of the shifted and unshifted probes with matrix polymers results in different diffusion coefficients for the two probes, which in turn gives rise to the decay–growth–decay type signal.

Computer simulations of these abnormal FRS signal shapes with complementary grating effect have been provided by Rhee et al.[11] and Huang et al.[17] More recently, the effect of complementary grating on apparent diffusion coefficient has been examined in detail by Park et al. with use of detailed simulation studies.[1] An experimental verification of the proposed effect however is yet to be established.

The objective of this study is to test the hypothesis of complementary double grating effect by means of a critical comparison of the diffusion coefficient deduced by a new analysis method proposed herewith for complex FRS signals with that by another independent means, e.g., dynamic light scattering (DLS).[20] In this report, we present the results of FRS and DLS studies on bovine serum albumin–sodium dodecyl sulfate (BSA–SDS) complexes. By varying the surfactant to protein ratio, we can produce FRS signal decay profiles with extreme departures from the single exponential, such as decay–growth–decay type. Unlike monotonic decays of single or multiple exponential, this kind of profile allows us to determine quite reliably the diffusion coefficient. Thus, the new analysis scheme proposed here is to exploit the complex features of such FRS signals. In so determining the diffusion coefficients by FRS, we can subject them to a critical comparison to those determined by DLS.

† University of Wisconsin.
‡ POSTECH.

0024-9297/93/2226-3086$04.00/0

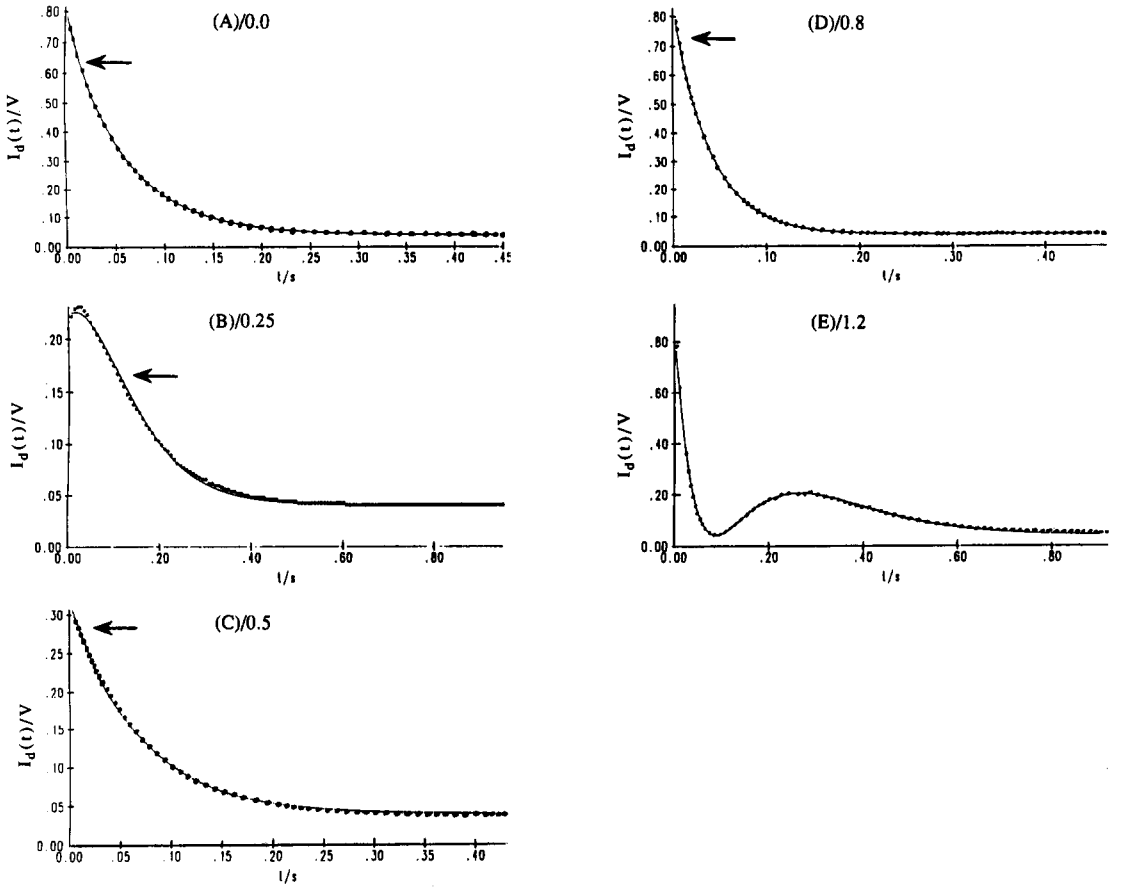

Figure 1. FRS profiles obtained at different SDS/BSA mass ratios: (A) zero, (B) 0.25, (C) 0.5, (D) 0.8, and (E) 1.2. The progressive change in the shape of decay profile is evident. The solid curves are the best fit results according to eq 1, with the fixed mean τ's inferred from DLS results for A–D and with the fixed mean τ from the Δt method for E (see text for details). Filled arrows indicate the starting points of forced fit to a single exponential function.

Analysis of Decay–Growth–Decay Signal

In the limit of pure-phase or amplitude grating,[7,8] the diffracted intensity from such a complementary pair of gratings follows the form

$$I_d(t) = [A_1 \exp(-t/\tau_1) - A_2 \exp(-t/\tau_2)]^2 + B \quad (1)$$

where τ_1 and τ_2 are decay time constants of two complementary gratings, B is the base line, and A_1 and A_2 represent the amplitude of optical fields diffracted from the complementary pair. Analysis of such a decay profile with five unknown parameters is nontrivial. On the basis of eq 1, the optical field amplitude of one of two complementary gratings must predominate, if the two decay constants are different, in order to observe a single exponential decay: $A_1 \gg A_2$ or $A_1 \ll A_2$ if $\tau_1 \neq \tau_2$. Otherwise, the decay profile shows a deviation from a single exponential form.[1] One of the frequently observed extreme departures, i.e., a decay–growth–decay type signal as shown in Figure 1E, has been analyzed either by a stripping method[11] or by profile fitting through a nonlinear regression scheme to the model function of eq 1.[13,17,18] However, the results of such nonlinear regression analyses are prone to depend on initial guesses for the fitting. This problem has been recognized, and a most reasonable set of τ_1 and τ_2 had to be selected among several equally acceptable results of the regression analysis.[18] Here we put forth an alternative method to analyze the decay–growth–decay type of signals, which is subject to a lesser degree of ambiguity.

For this type of signal, the dip and maximum occur at t_{min} and t_{max}, respectively, satisfying the following conditions arrived at by differentiation of eq 1 with respect to t.

$$A_1 \exp(-t_{min}/\tau_1) = A_2 \exp(-t_{min}/\tau_2) \quad (2)$$

and

$$A_1/\tau_1 \exp(t_{max}/\tau_1) = A_2/\tau_2 \exp(-t_{max}/\tau_2) \quad (3)$$

Eliminating A_1 and A_2 by dividing eq 3 by eq 2, we can obtain

$$\ln(\tau_2/\tau_1) = -(t_{max} - t_{min})(1/\tau_2 - 1/\tau_1) \quad (4)$$

and

$$\Delta t \equiv t_{max} - t_{min} = \frac{\ln\left(\frac{\tau_2}{\tau_1}\right)}{\left(\frac{1}{\tau_1} - \frac{1}{\tau_2}\right)} \quad (5)$$

It can be shown that Δt in eq 5 approaches the geometric mean of τ_1 and τ_2, i.e., $\Delta t \approx (\tau_1\tau_2)^{1/2}$ when the difference between τ_1 and τ_2 is small compared to individual values of τ_1 and τ_2. Such is a readily attainable condition for the case of azobenzene-labeled macromolecules since azobenzene moiety undergoes photochromic *cis–trans* isomerization, giving rise to a small difference in the diffusion coefficients of the macromolecules with *cis* and *trans* isomers of the photolabel. Under such a circumstance, Δt can be used in place of τ_1 and τ_2 to obtain the mean diffusion coefficient for the subsequent analysis, such as q^2 dependence, where q is the magnitude of scattering momentum transfer, $q = 2\pi/d$ with d being the fringe spacing.

Experimental Section

Materials. BSA (Pentex Brand Monomer Standard, ICN Biomedical) has been used after labeling with a photochromic dye, *p*-(phenylazo)phenyl isothiocyanate (Fairfield Chemical). 2-mercaptoethanol, EDTA disodium salt, and SDS were used as received from Sigma. The BSA sample was received as a lyophilized form, and the vendor specified that the sulfhydryl groups were reacted with L-cystine to remove any possibility of polymerization among BSA molecules, but they also noted that the sample includes some oligomers formed during the drying process. We found from PAGE (polyacrylamide gel electrophoresis) without SDS that the sample is 65.4% monomer, 26.3% dimer, 7% trimer, and traces of higher oligomers, while PAGE with SDS showed a clean single band. Since the oligomers break up upon addition of SDS, the oligomers were thought to be aggregated by physical forces, not by any chemical reactions. A majority of the experiments deals with BSA–SDS complexes and it is expected that the polydispersity at the globular state of BSA may be of little consequence; hence, no effort was made to fractionate the protein. The labeling procedure of BSA is practically the same as that described previously,[21] except that 20 mM phosphate buffer at pH 9.3 was used to improve the labeling efficiency. After the purification of labeled BSA by a Sephadex G-25 column and dialysis with 0.1 M phosphate buffer at pH 6, its labeling content was determined from the optical absorbance at 360 nm with use of a calibration curve obtained with the same dye attached to a free amino acid, lysine. The protein concentration was also determined by spectrophotometry from the absorbance at 278 nm after correcting for the absorbance of the dye at the same wavelength. The molar ratio of labeled dye to BSA was found to be 4.4. Sample solutions for FRS and DLS contain 0.5 wt % of BSA, 0.15% of 2-mercaptoethanol, 2 mM EDTA, and an appropriate amount of SDS in 0.1 M phosphate buffer at pH 6.

Methods. The experimental details of DLS and FRS have been described elsewhere,[22,23] and all of the experiments were performed at 25 °C. The DLS measurements were carried out at six different scattering angles from 40° to 130°, and the autocorrelation functions of the scattered signals were analyzed by fitting to two model functions, a single exponential function and a second-order cumulant function. Normally, the latter analysis yielded a better fitting result although the difference between the two did not amount to more than a few percent. In view of such a small difference and relative to FRS analyses given below, we present only those DLS results analyzed by fitting to the single exponential model function. The FRS data were analyzed by two methods. For a simple "exponential looking" decay, a non-linear regression analysis routine by the Marquardt algorithm is employed with the typical model function,

$$I_d(t) = [A \exp(-t/\tau) + B]^2 + C \qquad (6)$$

and the apparent diffusion coefficients are determined from a $1/\tau$ vs q^2 plot. When a decay–growth–decay type profile is evident, the Δt was determined directly from the decay profile and the diffusion coefficient was obtained from its q^2 dependence, which is a clear consequence of $\Delta t \approx (\tau_1\tau_2)^{1/2}$. We call this way of determining the diffusion coefficient henceforth the "Δt-analysis".

Results and Discussion

We chose the BSA–SDS complex labeled with *p*-(phenylazo)phenyl isothiocyanate as our test system since (1) the changeover of the FRS decay profile from a single exponential to an after-pulse-rise to a decay–growth–decay type is observed upon addition of SDS, (2) the azobenzene derivative shows a negligible absorption at the reading beam wavelength so that nearly a pure phase grating is expected, which justifies the use of eq 1, (3) only a slight difference in the diffusion coefficients of BSA–SDS complex containing *cis* and *trans* isomers of azobenzene moiety is expected, and (4) the diffusion coefficients of BSA–SDS complex can be measured with sufficient precision by an alternative method, namely dynamic light scattering.[20]

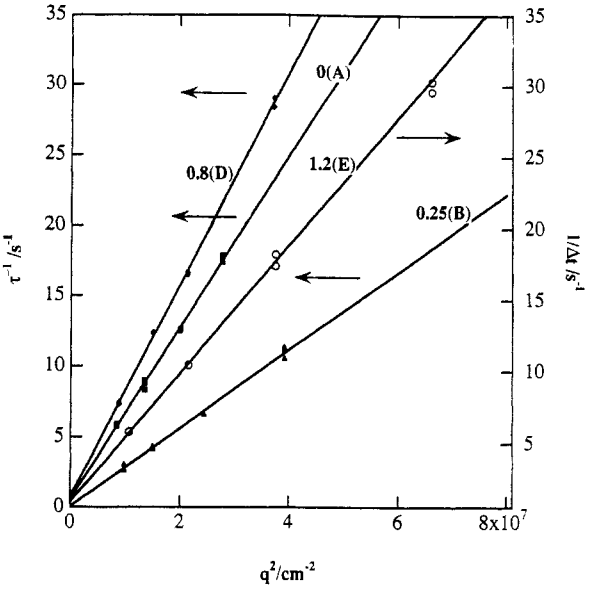

Figure 2. q^2 dependence of the decay time constant, τ and the lapse time, Δt. The τ's are determined by fitting to eq 6 from the signal shapes as shown in Figures 1A–D, with the SDS/BSA mass ratio designations being the same. The open circles represent the q^2 dependence of Δt determined from Figure 1E. The data at SDS/BSA = 0.5 are deleted for the purpose of clarity.

In Figure 1 are shown the FRS profiles of labeled BSA at five different SDS concentrations. The numbers on the top of the figures indicate the mass ratio of SDS/BSA. It is clearly seen that the FRS signal shape gradually changes upon addition of SDS. The FRS signal shape without SDS is almost an ideal single exponential decay, and the decay constant is deduced according to eq 6. As shown in Figure 2, a reasonable linear scaling with q^2 for $1/\tau$ is obtained, and the diffusion coefficient so determined is comparable to but slightly smaller than that by DLS. With the addition of SDS, the initial decay portion of profile becomes broader with a simultaneous decrease of the apparent diffusion coefficient. As SDS concentration increases further, the initial decay gets faster and eventually the decay–growth–decay profile starts to develop when the mass ratio SDS/BSA exceeds 1.2. It is most noteworthy that the signal intensity at the dip position of the decay–growth–decay signal fully reaches the null point, showing that two complementary gratings are almost 180° out of phase with each other. When such a decay–growth–decay profile is evident (SDS/BSA $\geq$ 1.2), the Δt-method is used, and a reasonable q^2 dependence is apparent for this type of signals, as shown in Figure 2E.

In Figure 3 are plotted the diffusion coefficients of the SDS–BSA complexes as a function of SDS/BSA ratio. The abscissa represents the mass ratio of SDS/BSA, and the top scale shows the molar ratio of SDS/amino acid residue; an average amino acid molar mass of 114 was used to calculate the ratio. The diffusion coefficients determined by DLS are represented by open squares. The filled circles represent the diffusion coefficients of the complexes at SDS/BSA < 1.2, where the signal follows an apparently single exponential decay. The diffusion coefficients of the complexes with this type of signal profiles were deduced by fitting the signal to eq 6. We call this way of determining the diffusion coefficient henceforth the "routine" analysis. The open circles represent the diffusion coefficients of the complexes at SDS/BSA $\geq$ 1.2, where the signals are of decay–growth–decay type, and the diffusion coefficients of the complexes with decay–growth–decay type signal

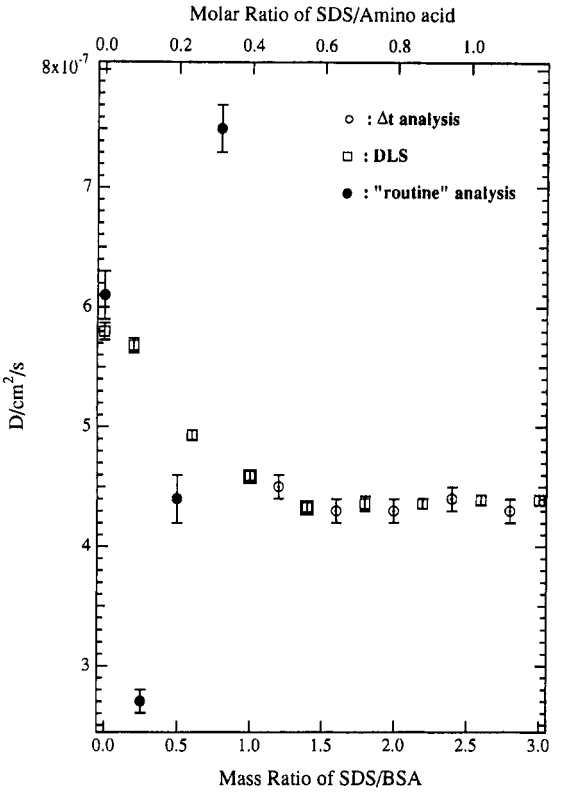

Figure 3. Diffusion coefficient of BSA–SDS complex determined by FRS and DLS. The open circles represent the FRS results analyzed by Δt analysis, the closed circles are the FRS results by "routine analysis", i.e., analysis by forced fitting to eq 6, and the open squares are the DLS results obtained by fitting to a single exponential function. The "routine analysis" shows large deviations from DLS results, while the Δt method with a decay–growth–decay type signal yields consistent results.

were determined by the Δt analysis. We now turn to the discussion of several points raised in these results.

FRS Signal Shape Change with SDS Concentration. In the range of SDS/BSA mass ratio of 0–1.2, it is clear that the diffusion coefficients of the complexes deduced by the routine analysis show significant deviations from those by DLS. As is manifested in Figure 2, q^2 dependence alone cannot be taken as a sufficient condition to ensure the correct analysis. We also tried to fit the signals with an intermediate SDS/BSA ratio by fixing the average decay time constant which is estimated from the DLS results as interpolated from the plot in Figure 3, and performing the three-parameter fit of the FRS profiles according to eq 1. The results of this fitting method are represented by the solid curves A–D in Figure 1, where the starting point of the fit for each profile is indicated by an open arrow. We emphasize two points from these analyses: (1) unambiguous determinations of the decay time constants are almost impossible even for the apparently single exponential decay, and (2) we can demonstrate clearly that the observed profile is successfully simulated by eq 1 with the use of decay time constants deduced by another method. This situation is exactly the expected behavior caused by the presence of the complementary concentration fringes decaying with different rates.[1] It illustrates the point that one has to be wary of pitfalls in the interpretation of a monotonically decaying profile since many different sets of the decay constants reproduce the entire profile rather successfully. To put it another way, it is much more difficult to deduce correctly the decay constants from a monotonic profile unless it falls into the exceptional case of purely single exponential decay or of well-separated multiexponential.

We now try to understand the signal shape change in Figure 1 and the deviation of the diffusion coefficients determined by the routine analysis from that determined by DLS in the intermediate SDS/BSA range. In the report by Park et al.,[1] the simulations of eq 1 were performed with A_1/A_2 fixed at 1.12 while varying the ratio of the two decay time constants τ_1/τ_2, and the results showed that the signal exhibits an after-pulse-growth when τ_1 is larger than τ_2, and that the signal changes to the decay–growth–decay type as τ_1 gets smaller than τ_2. Since the diffraction amplitude of the *trans* form of azo dye is expected to be larger than that of the *cis* form,[1] the results shown in Figures 1 and 3 can be accounted for by the complementary grating effect as follows. Initially in the absence of SDS, D_{trans} appears to be the same as D_{cis}, judging from the similarity between the diffusion coefficient of dynamic light scattering, D_{DLS}, and that of forced Rayleigh scattering, D_{FRS}, in Figure 3. With addition of SDS, D_{trans} gets smaller and the signal exhibits a distinct after-pulse-rise (B). The apparent diffusion coefficient of FRS drops accordingly to show a negative deviation from that of DLS. Upon addition of more SDS, the difference starts to become smaller and the after-pulse-rise shape becomes less distinct (C). At a point between C and D the reversal in the magnitudes of D_{trans} and D_{cis} takes place, and the apparent diffusion coefficient becomes larger than that of DLS. Finally, the difference becomes large enough to develop a visible bump (E). We will present in the last section our conjecture on how the *cis* and *trans* forms of the azo dye affect the conformation and diffusion coefficient of the complex and why the reversal of D_{trans} and D_{cis} takes place with the known BSA denaturation mechanism by SDS.

D_0 of Globular BSA without SDS. We now revisit the diffusion coefficient of BSA in the infinite dilution limit D_0 without SDS. Our value is smaller than the ones reported in the literature. The generally accepted value for BSA diffusion coefficient in the literature is 6.0×10^{-7} cm²/s at 20 °C or 6.8×10^{-7} cm²/s at 25 °C.[24-26] Honda and Kambe[27] recently reported that D_0 at 25 °C is 6.71×10^{7} cm²/s for well-fractionated BSA monomer, 6.1×10^{-7} cm²/s for unfractionated BSA, and 5.2×10^{-7} cm²/s for fractionated BSA dimer. Hence, the smaller diffusion coefficient of BSA without SDS in this experiment appears to be the result of the polydispersity of our sample. We also note that the signal at SDS/BSA = 0 is not a decay–growth–decay type but a single exponential one, as shown in Figure 1A. This is contrary to what Stewart et al.[12] observed with ABITC–IgG. It was proposed by the authors that when they labeled the protein with the azo dye at pH 11.3, the labeling reaction caused aggregation of the protein and the FRS signals from ABITC–IgG showed the decay–growth–decay shape. The authors further attributed the occurrence of this signal to the photodissociation of the protein aggregation upon photoexcitation of the dye. Because the FRS signal shape of ABITC–BSA in this experiment is single exponential, we argue that the presence of aggregates does not necessarily produce a decay–growth–decay type signal. Arunyawongsakorn et al.[26] also reported a single exponential decay signal from monomeric BSA labeled with ABITC. The diffusion coefficient they deduced from these signals is comparable to the generally accepted value. Thus, our claim of no complementary grating effect for ABITC–BSA without SDS accords with the latter observation, but the diffusion coefficient of our sample is smaller than theirs by 15%, probably due to the polydispersity of our sample. The presence of oligomers may also explain the slightly smaller value of the diffusion coefficient determined by DLS than

the one determined by FRS: DLS probes the z-average diffusion coefficient, and it is very sensitive to the small amount of large scatterers, whereas FRS signal intensity is only proportional to the number of photosensitive molecules attached to the oligomers; hence, the diffracted probe beam intensity is not as sensitive to large oligomers as the scattered laser intensity in DLS.

D_0 of BSA–SDS Complexes. Secondly, we not that the diffusion coefficients determined by the Δt analysis at SDS/BSA $\geq$ 1.2 are in good agreement with those determined by DLS within experimental uncertainty. The aggreement is consistent with our proposal that the geometric mean of two slightly different decay time constants equals Δt. The linear q^2 dependence of Δt in Figure 2E may be taken as further evidence that the Δt is related to some decay time constants connected to translational diffusion processes. Additionally, the diffusion coefficients of BSA–SDS complexes at SDS/BSA $\geq$ 1.2 are also in good agreement with the one reported by Honda and Kambe,[27] $4.3(\pm0.2) \times 10^{-7}$ cm^2/s. Because they used a fractionated BSA sample, the agreement between ours and theirs indicates that only the complexes with monomeric BSA are present in our samples when SDS is added, even though the globular state may be polydisperse. It also supports the expectation as noted earlier that the oligomers are not covalently linked but aggregated through some physical means which are susceptible to breakup by SDS. Given the average decay time constant from Δt, a nonlinear regression analysis was carried out under the constraint of $(\tau_1\tau_2)^{1/2} = \Delta t$. We found that the fit results are well reproducible, virtually independent of the initial guesses. The best fit results are shown in Figure 1E with the solid curve, and the quality of fit is indeed satisfactory. By so fitting, we could obtain all the parameters in eq 1; for instance, at BSA:SDS = 1:1.2, $\tau_1 = 0.172$ s, $\tau_2 = 0.180$ s, $A_1 = 33.2$, and $A_2 = 32.3$, indicating that the diffraction efficiencies of two complementary gratings are so similar that only a percent of the diffraction intensity is being detected because of the mutual interference of the diffraction signals from the complementary gratings. Under this circumstance, only about 5% difference in the decay rates results in such a drastic departure from a single exponential on the FRS decay profile. Assuming that the contrast between two complementary gratings is an inherent property of the photolabel species used in this experiment and further the contrast remains unaffected by SDS concentration, we infer that the difference in the diffusion coefficients of BSA–SDS complexes having *cis* and *trans* form of the dye varies in a complicated manner with added SDS however small.

Effect of Azo Dye on BSA Denaturation. The denaturation of protein by SDS is known to take place in a stepwise fashion.[28–30] It is believed that the protein has a cleft between two globular units, wherein are embedded 40 lysil and 40 carboxyl residues, and that these residues become exposed when the protein has a high net charge.[28] The SDS molecules bind first to the positively charged and exposed (toward aqueous medium) residues by ionic interactions, followed by the hydrophobic binding of the surfactant molecules to the newly exposed hydrophobic segments. The reversal in the magnitude of D_{trans} and D_{cis}, which was manifested by the signal shape change in Figure 1 and by the change from the negative deviation of D_{FRS}, relative to D_{DLS}, to the positive deviation in Figure 3, might be an indication of this stepwise denaturation. Our speculation is that because the dipole moment of the *trans* form is much smaller than that of the *cis* form,[2] the *trans* can penetrate more easily into the hydrophobic part of the protein, thus altering the compact structure of the protein, which in turn makes it easier for SDS molecules to effect the N–F-type transition of the protein. The result would be a larger size and smaller diffusion coefficient of the complex with the *trans* form in an early stage of denaturation. Once the protein unfolds, however, the BSA–SDS complex is believed to be a string of micelles, like a necklace,[31] and the more hydrophobic and linear *trans* form would result in a tighter binding with the micelles, which in turn would produce a smaller size and larger diffusion coefficient of the complex. In other words, it appears that the complex with the *trans* form of the dye molecule has a larger size than the one with the *cis* form in the first stage of denaturation, but that the size of the complex with the *trans* form becomes smaller than the one with the *cis* form as the protein denaturation gets into the second stage, where SDS molecules bind to the protein mainly by hydrophobic interactions. If this is indeed the case, then the first stage of SDS binding is apparently complete at SDS/BSA ratio at 0.25–0.5, judging from the attending increase in the apparent diffusion coefficient, D_{FRS}. The positive deviation of D_{FRS} from D_{DLS} increases with SDS/BSA ratio, until the difference between D_{trans} and D_{cis} is large enough to produce a decay–growth–decay type signal at SDS/BSA = 1.2. When the average diffusion coefficient settles down to a constant value, $4.4(\pm0.1) \times 10^{-7}$ cm^2/s, at SDS/BSA $\geq$ 1.4, the signal shape also remains unchanged, indicating the completion of SDS binding to the protein. The stepwise denaturation mechanism, suggested here, is supported by some experimental results. Tipping et al.[28] reported that the specific viscosity increases little up to SDS/BSA = 0.35 and then increases sharply thereafter, and the reaction enthalpy also increases sharply at SDS/BSA $\geq$ 0.52. Equilibrium binding studies by Takeda et al.[29] showed that the onset of the second stage binding is also at SDS/BSA = 0.52. The NMR study by Oakes[30] also showed that the chemical shift of the CH_3 and α-methylene groups of SDS starts to increase at SDS/BSA = 0.43. Therefore, the FRS signal shape change being reported here is not only an indication of different diffusion coefficients of the complexes with the two configurational forms by the azo dye but also lends support to the stepwise denaturation mechanism of BSA by SDS.

It would be pertinent to discuss briefly the results from this study vis-a-vis other existing results. The studies of Reynolds and Tanford indicated that various globular proteins, with reduced disulfide bonds, appear to bind an identical amount of SDS, i.e., 1.4 g of SDS/g protein, and suggest a rodlike structure for the protein–SDS complex based on the hydrodynamic properties of the complex.[32,33] As shown in Figure 3, the diffusion coefficient of BSA/SDS complex decreases sharply upon addition of SDS and reaches an asymptote at near 1.4 g SDS/protein, which is in excellent accord with the result from the equilibrium binding studies with respect to the saturation binding ratio. A more recent DLS study by Tanner et al.[34] showed a similar decrease of the diffusion coefficient of BSA/SDS complex as the concentration of SDS was increased while their saturation limit was 2.8 g of SDS/g of protein. They observed apparently double exponential autocorrelation functions of DLS signals and interpreted the results by invoking coexistence of SDS micelles and the complexes. We also observed a similar non-single exponential autocorrelation function at low ionic strength as they used, i.e 20 mM; however, at high ionic strength a clean single exponential form was obtained in 100 mM phosphate buffer at pH 6. It suffices here to point out that the apparent diffusion coefficient at low ionic strength is

Table I. Comparison of Decay Time Constants by Nonlinear Regression and Δt Analyses

system	τ_1	τ_2	$(\tau_1+\tau_2)/2$	$(\tau_1\tau_2)^{1/2}$	Δt[a]
benzospiropyran-BSA[b]	0.16	0.4	0.28	0.25	0.23
CQ/PMMA[c]	25.2	80	52.6	44.9	40
CQ/PMMA[d]	43.3	162	103	83.8	72.1
CQ/PC[e]	418	2800	1609	1082	848
CQ/PS[f]	1493	1667	1580	1578	1545

[a] The time interval between the maximum and the minimum intensities of "decay-growth-decay" signals. [b] Reference 11. [c] Reference 14, CQ stands for camphor quinone and PMMA for poly(methyl methacrylate). [d] Reference 15. [e] Reference 16, PC stands for polycarbonate. [f] Reference 13, PS stands for polystyrene.

subject to a variety of polyelectrolyte effects,[35] hence, DLS is not an appropriate probe to deduce the size of highly charged species such as protein/SDS complexes unambiguously.

Comparison of Δt with Average Decay Constant. We now test our proposal with the extant data in the literature. In Table I are collected the data from five decay-growth-decay type signals in the literature. The values of τ_1 and τ_2 are originally reported ones, and the arithmetic and geometric averages, $(\tau_1+\tau_2)/2$ and $(\tau_1\tau_2)^{1/2}$, respectively, in columns 3 and 4 were calculated from the original data. The time interval Δt was determined from the minimal and maximal intensity points in the reported figures. We first note that the Δt is indeed close to the geometric average, even when the two decay time constants are separated by a factor of several. Secondly, Δt is closer to the geometric average than the arithmetic average, and the difference between them increases with the ratio τ_2/τ_1. These are exactly as expected, for the geometric mean is closer to Δt by simple series expansions; the arithmetic mean $(\tau_1+\tau_2)/2 = \tau_1 + \Delta\tau/2$, the geometric means $(\tau_1\tau_2)^{1/2} = \tau_1 + \Delta\tau - \Delta\tau/8\tau_1$, and the time interval $\Delta t = \tau_1 + \Delta\tau - \Delta\tau/6\tau_1$, where $\Delta\tau = (\tau_2 - \tau_1)$. Thus, it is not surprising that the difference between the geometric means and Δt is less than 20% when the ratio τ_2/τ_1 is smaller than 4, as seen in Table I. Therefore, the Δt analysis can be applied to virtually all the decay-growth-decay-type signals to deduce the geometric average of the diffusion coefficients with reasonable accuracy. The advantages of using the Δt analysis are that it provides the geometric mean of the two diffusion coefficients very accurately with virtually no effort and that the four-parameter fitting to eq 1, where B is generally negligible, is reduced to a three-parameter fitting by virtue of being able to fix $\tau_2 = (\Delta t)^2/\tau_1$, thus providing the fitting result more reliability.

Conclusions

In summary, we have shown that the complementary grating effect can be invoked successfully to account for complicated FRS signals and that the diffusion coefficients determined by the Δt analysis are within the experimental error the same as those by DLS. Comparison of the Δt and the geometric means $(\tau_1\tau_2)^{1/2}$ from the data reported in the literature also proved that Δt can be deduced reliably whereby we can reduce the fitting routine (to eq 1) to a three-parameter one in the common cases when the background term B is set to zero. What concerns us most in FRS studies is how one deals with nearly "normally looking" monotonic decays. As demonstrated in this study, a routine analysis of a normal single exponential decay is potentially fraught with a significant error in deducing the correct decay constant. We should like to close this report by calling attention to the proposition that one must bear in mind critical photochemical details of the chosen probes in order to arrive at the correct interpretations of FRS data.

Acknowledgment. This work is in part supported by the Polymers Program of NSF (DMR-8903943) and Eastman Kodak Company. T.C. acknowledges the financial support from the Korea Ministry of Education and Korean Science and Engineering Foundation.

References and Notes

(1) Park, S.; Sung, J.; Kim, H.; Chang, T. *J. Phys. Chem.* **1991**, *95*, 7121.
(2) Urbach, W.; Hervet, H.; Rondelez, R. *J. Chem. Phys.* **1985**, *83*, 1877.
(3) Kim, H.; Chang, T.; Yohanan, J. M.; Wang, L.; Yu, H. *Macromolecules* **1986**, *19*, 2737.
(4) Antonietti, M.; Coutandin, J.; Grütter, R.; Sillescu, H. *Macromolecules* **1984**, *17*, 798.
(5) Tran-Cong, Q.; Chang, T.; Han, C. C.; Nishijima, Y. *Polymer* **1988**, *29*, 2261.
(6) Nemoto, N.; Kishine, M.; Inoue, T.; Osaki, K. *Macromolecules* **1990**, *23*, 695.
(7) Kogelnik, H. *Bell Syst. Tech. J.* **1969**, *48*, 2909.
(8) Nelson, K. A.; Casalegno, R.; Miller, R. J. D.; Fayer, M. D. *J. Chem. Phys.* **1982**, *77*, 1144.
(9) Barish, A.; Bradley, M. S.; Johnson, C. S., Jr. *Rev. Sci. Instrum.* **1986**, *57*, 904.
(10) Chang, T.; Kim, H.; Yu, H. *Chem. Phys. Lett.* **1984**, *111*, 64.
(11) Rhee, K. W.; Gabriel, D. A.; Johnson, C. S., Jr. *J. Phys. Chem.* **1984**, *88*, 4010.
(12) Stewart, U.; Johnson, C. S., Jr.; Gabriel, D. A. *Macromolecules* **1986**, *19*, 964.
(13) Zhang, J.; Wang, C. H. *J. Phys. Chem.* **1986**, *90*, 1299.
(14) Zhang, J.; Yu, B. K.; Wang, C. H. *J. Phys. Chem.* **1986**, *90*, 2296.
(15) Zhang, J.; Wang, C. H.; Ehlich, D. *Macromolecules* **1986**, *19*, 1390.
(16) Wang, C. H.; Xia, J. L.; Yu, L. *Macromolecules* **1991**, *24*, 3638.
(17) Huang, W. J.; Frick, T. S.; Landry, M. R.; Lee, J. A.; Lodge, T. P.; Tirrel, M. *AICHE J.* **1987**, *33*, 573.
(18) Lee, J. A.; Lodge, T. P. *J. Phys. Chem.* **1987**, *91*, 5546.
(19) Lee, J.; Park, K.; Chang, T.; Jung, J. C. *Macromolecules* **1992**, *25*, 6977.
(20) For an example, see: Pecora, R., Ed. *Dynamic Light Scattering*; Plenum: New York, 1971.
(21) Kim, H.; Chang, T.; Yu, H. *J. Phys. Chem.* **1984**, *88*, 3946.
(22) Wang, L.; Garner, M. M.; Yu, H. *Macromolecules* **1991**, *24*, 2368.
(23) Wesson, J. A.; Noh, I.; Kitano, T.; Yu, H. *Macromolecules* **1984**, *17*, 782.
(24) Oh, Y. S.; Johnson, C. S., Jr. *J. Chem. Phys.* **1981**, *74*, 2717.
(25) Raj, T.; Flygare, W. H. *Biochemistry* **1974**, *13*, 3336.
(26) Arungyawongsakorn, U.; Johnson, C. S., Jr.; Gabriel, D. A. *Anal. Biochem.* **1985**, *146*, 265.
(27) Honda, C.; Kambe, Y. *J. Chem. Soc. Jpn.* **1988**, 194.
(28) Tipping, E.; Johns, M. N.; Skinner, H. A. *J. Chem. Soc., Faraday Trans. 1* **1974**, *70*, 1306.
(29) Takeda, K.; Miura, M.; Takagi, T. *J. Colloid Interface Sci.* **1981**, *82*(1), 38.
(30) Oakes, J. *J. Chem. Soc., Faraday Trans. 1* **1974**, *70*, 2200.
(31) Guo, X. H.; Zhao, N. M.; Chen, S. H.; Teixeira, J. *Biopolymers* **1990**, *29*, 335.
(32) Reynolds, A.; Tanford, C. *Proc. Natl. Acad. Sci. U.S.A.* **1970**, *60*, 1002.
(33) Reynolds, A.; Tanford, C. *J. Biol. Chem.* **1970**, *245*, 5161.
(34) Tanner, R. E.; Herpigny, B.; Chen, S.-H.; Rha, C. K. *J. Chem. Phys.* **1982**, *76*, 3866.
(35) Schurr, J. M.; Schmitz, K. S. *Ann. Rev. Phys. Chem.* **1985**, *37*, 271.